Distribution of Aortic Mechanical Prosthetic Valve Closure Sound Model Parameters on the Surface of the Chest

Ahmet Baykal, Y. Ziya İder, and Hayrettin Köymen, *Senior Member, IEEE*

Abstract— **It has been previously proposed that heart valve closure sounds can be modeled by a sum of decaying sinusoids, based on the hypothesis that the heart cavity, heart walls, major vessels, and other structures in the chest constitute a frequency selective linear acoustic system and this system is excited by the rapidly decelerating valve occluder. In this study, distribution of the parameters of this model for the second heart sound is investigated. For this purpose, heart sounds of 10 patients who have a St. Jude-type bileaflet mechanical heart valve prosthesis in aortic position are recorded. Recordings are performed at 12 different locations on the surface of the chest. To reliably assign representative parameters to each recording site, signal averaging, model order selection, and a special filtration technique are employed. The results of the analyses are discussed in relation to the above hypothesis on the heart sound generation mechanism. It is observed that site-to-site variation of frequencies of modes does not exceed the accuracy limit of proposed analysis method, but energies of these modes vary on the surface of the chest, and as a result of statistical analysis, it appears that energy of some modes are significantly different between two recording sites.**

I. Introduction

SPECTRAL analysis of the heart sound has been used by researchers for different purposes. Several investigators have reported that by using such a technique, anatomical or physiological malfunctions in heart valve prostheses can be differentiated [1]–[6]. It is also reported that power spectrum of the heart sound may vary in relation to certain cardiovascular disorders [7]–[11].

In all of those studies, different spectral parameters have been used. Gordon *et al.* used maximum frequency as a diagnostic criterion and they observed that mechanical malfunction of a heart valve prosthesis causes a decrease in this parameter [2]. Kagawa *et al.* have reported that the normalized maximum frequency (upper cut-off frequency 30 dB below the maximum) of power spectrum decreases during the postoperative course of patients with thrombosed valves [3]. Stein *et al.* studied patients with degenerated porcine bioprosthetic valves. They defined "dominant frequency" as the frequency of the highest magnitude shown in the sound spectrum. They reported that this parameter is higher in patients with degenerated heart valve prosthesis than that in normal subjects [5]. In a recent study, Durand *et al.* extracted 18 diagnostic features from the sound spectrum and they used these parameters to distinguish subjects with normal valves from those with degenerated valves [6].

In most of these studies, investigations have been based on some heuristic features derived from the power spectrum. Variations of these heuristic features have been analyzed between subjects with normal valves and those with degenerated valves. These features are not related to the parameters of a particular model which attempts to explain the heart sound generation mechanism. Therefore, it is difficult to use these features for a better understanding of heart sound generation mechanism. If, however, parameters of a model which has been built by considering the influence of anatomical and physiological factors on heart sound generation were used, then better understanding of heart sound generation and better diagnosis of pathological situations would be achieved. Especially in follow-up studies, model-based approaches can be more sensitively used to follow the development of pathology [12].

Several different views about sound generation mechanisms have been adopted by different investigators. Sikarskie *et al.* proposed a mathematical model for aortic valve vibration and its relation to the second heart sound [13]. But they did not undertake a study to verify this model using PCG signals. Furthermore, this model only considered a valvular origin for heart sound, whereas other investigators emphasize the contribution of the oscillating structures in the chest [7], [10], [14]. However, they did not formulate mathematical models to explain their assumptions. As an extension to the emphasis put by these investigators, it was assumed in a recent study that heart sounds are generated as a response of a frequency-selective linear-acoustic system to the rapidly decelerating heart valve occluder [12]. It is considered that this system consists of the entire heart cavity, heart walls, major vessels, and other structures in the chest, all having natural resonance modes. In line with this hypothesis, heart sounds are expressed as a summation of damping sinusoids. Although a detailed correspondence between the parameters of this model and anatomical and physiological factors was not established, it was nevertheless shown that by estimating the parameters using Prony estimation technique [15], a good fit

Manuscript received August 19, 1991; revised February 19, 1993 and December 19, 1994.

A. Baykal and Y. Z. İder are with the Department of Electrical and Electronics Engineering, Middle East Technical University, 06531 Ankara, Turkey.

H. Köymen is with the Electrical and Electronics Engineering Department, Bilkent University, 06530 Ankara, Turkey.

IEEE Log Number 9409107.

was obtained between the model parameters and actual heart sound signal.

In order to verify a model, it is necessary to test on a quantitative basis the implications of the hypotheses which stem from the specific assumptions about the heart sound generation mechanisms themselves. For example, if the resonant structure assumption is true, then frequencies of these resonance modes will not vary from one recording site to another on the surface of the chest, but the energy content of these modes will be different depending on the distances of the recording sites to the anatomical structures having natural resonance modes. It must be emphasized that such a hypothesis can not be tested using the above-mentioned heuristic features of the power spectrum of the heart sound. For example, frequency of peak amplitude of the power spectrum may change due to a change in the energies of the contributing resonance modes and not due to a change in their frequencies.

The purpose of this study is to investigate the variation of the modal parameters of second heart sounds on the chest surface and to identify whether any variations are due to frequency shifts or energy variations of the individual damped sinusoids on different recording sites. Closure sounds originating from metallic prosthetic valves are particularly suitable for such an investigation since the rapid deceleration of the valve occluder provides excitation, which has a wide frequency spectrum, to the acoustic system, comprising heart, major vessels, and other structures in the chest [12]. Furthermore, the aortic component in this sound is very high compared to the pulmonary one, hence the interference effect of the latter is considerably less.

In this study, heart sounds are recorded from 10 patients who have a St. Jude-type bileaflet mechanical heart valve prosthesis in aortic position. Heart sounds are recorded at 12 different sites on the surface of the chest. Second heart sounds are selected and analyzed. Estimated parameters for each site are compared. Such a comparison requires a precise method for parameter identification. For this purpose, an algorithm is developed which aims at reliably assigning representative parameters to a given specific recording site, despite noise and some physiological variation. Signal averaging is employed and a model order selection procedure and special filtration technique are proposed. The results of the analyses are discussed.

II. Methods

A. Recording

Heart sounds of 10 patients who have St. Jude-type bileaflet mechanical heart valve prostheses implanted in aortic position, are recorded and second heart sounds are selected for analysis. Recordings are made by a Nihon Kohden (model RS5) PCG amplifier with -3 dB cutoff frequencies measured to be at 100 and 1940 Hz, and with 18 dB/octave fall-off outside the pass-band. The PCG transducer is of piezoelectric type (air coupled, Electronics for Medicine Inc., No. 03040502) and has a flat response in the range of frequencies mentioned above. Electrocardiograms are simultaneously recorded to be able to locate the second heart sound which occurs after the T wave.

The outputs of the PCG and ECG amplifiers are recorded by a multichannel FM tape recorder which has a 0–5 kHz flat frequency response. At playback, PCG signals are low-pass filtered (-48 dB/octave) at 500 Hz to prevent frequency aliasing. PCG and ECG are subsequently sampled and digitized by a 12-b A/D converter at a rate of 2 kHz and stored on diskettes. An IBM PC/AT personal computer is used to control data acquisition procedures and for off-line analysis. Operator interactive signal monitoring software displays the recorded PCG and ECG for a few cardiac cycles. One of the second heart sounds is selected as a template and the other second heart sounds are detected and aligned using cross-correlation for signal averaging purposes. In each recording site, 2–9-s heart sounds, which have more than 90% correlation with the reference template, are selected and then averaged. Averaged second heart sounds are then analyzed.

B. Parameter Identification

In this study, second heart sounds are modeled as the sum of decaying sinusoids (modes). In this model, if x_n represents the heart sound sampled at the nth sampling instant, then x_n is expressed as

$$x_n = \sum_{k=1}^{K} A_k \exp(-\alpha_k nT)\mathrm{Cos}(2\pi f_k nT + \Theta_k) + e_n \quad (1)$$
$$n = 1, \ldots, N$$

where

- N is the number of samples,
- K is the number of modes,
- A_k is the amplitude of the kth mode,
- α_k is the damping constant of the kth mode,
- f_k is the frequency of the kth mode,
- Θ_k is the phase of the kth mode,
- T is the sampling interval,
- e_n is the noise at the nth time instant.

The amplitude, damping constant, frequency, and phase of each mode are estimated by recursive implementation of the Prony method. SER_K which is defined as

$$\mathrm{SER}_K = 10\log\left(\left(\sum_{n=1}^{N} x_n^{*2}\right)\Big/\left(\sum_{n=1}^{N} e_n^{*2}\right)\right) \quad (2)$$

is the signal-to-error ratio (in dB) for a model having K modes, where

- x_n^* is the nth samples of estimated signal,
- e_n^* is the difference at nth sampling instant, between actual measurement and the prediction of the model (also called residual error).

Once the parameters of a model are identified, then the energy of the kth mode, E_k is calculated, using

$$E_k = \int_0^\infty A_k^2 \exp(-2\alpha_k t)\mathrm{Cos}^2(2\pi f_k t + \Theta_k)dt$$
$$= \frac{A_k^2(\alpha_k^2 + (2\pi f_k)^2 + \alpha_k^2\mathrm{Cos}2\Theta_k - 2\pi f_k \alpha_k \mathrm{Sin}2\Theta_k}{4\alpha_k(\alpha_k^2 + (2\pi f_k)^2)}. \quad (3)$$

TABLE I
PARAMETERS OF THE ARTIFICIAL CLOSURE SOUND

fre	damp	ampl	phase	energy
120	90	1000.0	4	1.000
170	100	985.4	0	1.000
220	150	1169.9	2	1.000

TABLE II
ESTIMATED PARAMETERS OF THE NOISELESS SIMULATED SIGNAL

fre	damp	ampl	phase	energy
120	90.1	1001.3	3.999	1.000
170	100.3	987.9	0.000	1.000
220	149.9	1170.1	2.001	0.999

1) Determination of the Model Order: Determination of the number of modes is of critical importance. We have done simulations to study the interrelations between mode number, parameter estimates, and the Signal-to-Noise ratio. A signal with three modes, the parameters of which are given in Table I, is generated and random sequences (zero mean, Gaussian sequence) of different variances are added to this signal. Thus, artificial closure sounds with SNR's of 21, 19, 15, 11, 8, 6, 4, and 0.5 dB are obtained. Here, SNR is defined as

$$\mathrm{SNR} = 10\log\left(\left(\sum_{n=1}^{N} x_n^2\right) \Big/ \left(\sum_{n=1}^{N} e_n^2\right)\right) \qquad (4)$$

where e_n is the random noise at the nth time instant.

All signals are analyzed at K of 3, 6, 10, 15, and 20. It is observed that if the signal is noiseless, correct parameters can be estimated at a K value of three (Table II). However, if the signal is noisy, accurate estimates (< 2% error for frequencies, < 10% error for relative energies of modes) can not be achieved when the model order is less then 10.

When Akaike Information Criterion (AIC) [16], which is a widely used method for order selection in AR models, is used in the AR modeling step of Prony technique to determine the model order, an order of five was indicated for all SNR used. This estimate is, of course, close to the number of poles in the AR model of a signal containing three decaying sinusoids. However, from the perspective of obtaining accurate estimates of parameters, the order determined by AIC was not sufficient.

In Fig. 1, SER_K of artificial closure sounds are shown. In this figure, the orders for which accurate estimates can be achieved are marked by "■." For these orders, estimation errors are between 0.1% and 2% for frequencies and 0% and 10% for relative energies. It can be seen from Fig. 1 that, as the model order is increased, SER_K increases. For a low noise case (SNR = 21 dB), the SER_K curve shows a sharp corner and reaches a plateau. This corner occurs at $K = 10$ and accurate frequency and energy estimation (< 2% error for frequencies, < 10% error for relative energies of modes) can be achieved for this and higher orders. For the signal for which SNR is 19 dB, the corner in the SER_K curve becomes smoother and accurate estimates can be achieved for K's of 15 and 20. In other cases for which SNR's are less than 19,

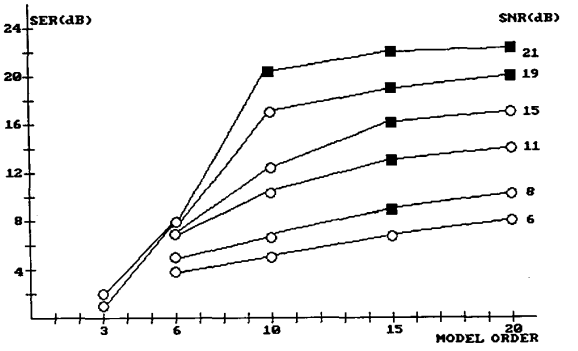

Fig. 1. SER_K curve of artificial closure sounds which are generated using the parameters given in Table I. The orders at which accurate estimates can be achieved are marked by "■" symbols. Accurate estimates can not be achieved at the orders marked by "○" symbols.

such a corner can not be observed. For the cases for which SNR's are between 19 and 6 dB, accurate estimates can only be achieved at K of 15. In the last case (SNR = 6 dB), no acceptable estimates can be found.

These observations imply that, when the noise level of the signal is sufficiently low, the SER_K curve shows a sharp corner. For the K value at which this corner occurs, accurate estimates can be achieved. If the noise level of the signals is relatively high, a corner in the SER_K curve can not be identified and, in these cases, using a high value of K does not necessarily yield correct parameter estimates. Indeed, if the model order is increased, SER_K increases, but the estimates become erroneous. Therefore, in the analysis of actual heart sounds, reduction of the noise level is of critical importance. For this purpose, signal averaging is found helpful.

For averaged heart sounds, the mode number is determined as follows: Signals are analyzed for increasing model orders, starting at $K = 6$. In each successive step, K is increased by two. As K is increased, SER_K increases and reaches a plateau. This curve may show a sharp corner depending on the level of noise. K for this corner is accepted as the model order. If such a corner can not be identified, the analysis is deemed invalid.

2) Filtration of Lower Frequency Modes: The principal aim of this study is to understand how the energies and frequencies of modes comprising a heart sound vary on the surface of the chest. The modeling and estimation techniques employed to this end must incorporate all precautions against the factors which reduce the precision of results. Apart from the effects of noise which are discussed in the previous section, signal components which can not be recorded with high fidelity are a serious concern.

Heart sound analyses used for clinical purposes are usually made in 100–200 Hz (for mid-frequencies) or 200–500 Hz (for high frequencies) [17]. For power spectrum analysis, different investigators have used different cut-off frequencies. For example, Arnott *et al.* used a band-pass filter with cut-off frequencies of 20 and 1500 Hz [10], on the other hand, Stein *et al.* recorded sound signals between 50–500 Hz [5]. Our PCG recording system has a high-pass filter with a −3 dB frequency of 100 Hz. However, most of the energy in the filtered signal

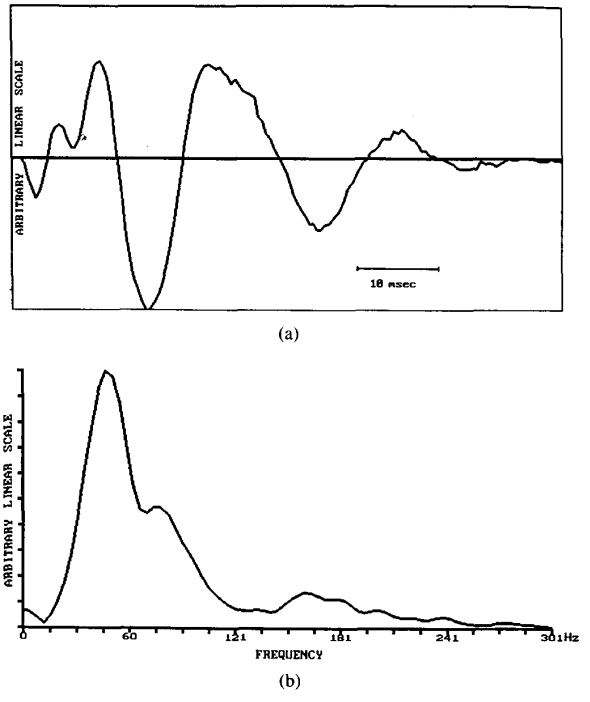

Fig. 2. (a) A typical closure sound. (b) DFT of this signal.

TABLE III
PARAMETERS OF THE CLOSURE SOUND GIVEN IN FIG. 3. ENERGIES ARE NORMALIZED TO THE ENERGIES OF THE MODES AT 99 HZ

fre	damp	ampl	phase	energy
37.7	97.1	9231.7	0.394	91.491
47.1	177.9	13283.7	3.864	72.184
55.1	94.4	6902.7	1.605	58.516
75.2	77.2	1296.8	1.844	2.824
99.3	103.5	1004.6	4.097	1.000
171.7	111.8	411.5	0.002	0.287
284.9	348.0	263.6	1.893	0.026

still lies below 100 Hz (Fig. 2). These components, on the other hand, do not lend themselves to a precise modal analysis because they are critically effected by the filter. In particular, minor variations in the modal frequency result in significant changes in modal energy if this signal component lies in the rising edge of the high-pass filter. Therefore, it is not appropriate to include these modes in our comparative study. Furthermore, the presence of these modes causes inaccuracies in the estimation of parameters of the components which are in the pass-band. Simulation studies were undertaken to demonstrate these effects.

For simulation purposes, an artificial closure sound is generated using (1) with $K = 7$ and the parameters shown in Table III which correspond to signals depicted in Fig. 2(a). e_n is selected as a zero-mean Gaussian sequence such that the SNR for this artificial signal is 22.5 dB.

The artificial signal is shown in Fig. 3. The Prony method is first applied to this signal without any prior filtering. The mode numbers are taken as 10, 12, 14, 16, 20, 22, and 24.

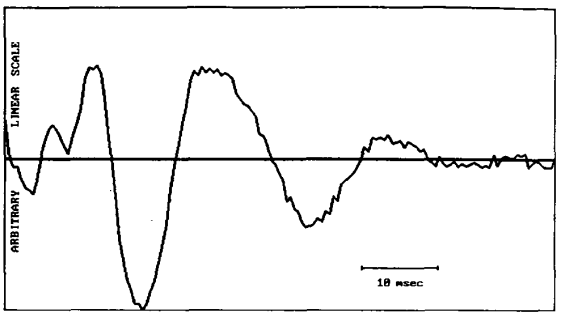

Fig. 3. Artificial closure sound which is generated using the parameters given in Table III.

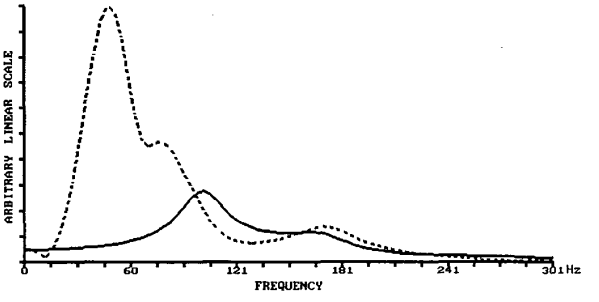

Fig. 4. DFT's of artificial closure sound, before (dashed line) and after (solid line) modal high-pass filtration.

The frequencies and energy of high-frequency modes can not be accurately estimated (error $< 2\%$ in frequency and $< 10\%$ in energy) in any of these cases. In fact, obtained errors are not even below 5% for frequencies and 25% for energies.

In this study, a special "modal high-pass filtering technique" is proposed in order to reduce the effect of low-frequency modes. The parameters of these modes to be minimized are estimated first in this technique. To do this correctly, the frequency band of the signal must be as small as possible for accurate estimation. On the other hand, it must be large enough to cover most of the energy contained in significant low frequency modes. We chose this frequency as 140 Hz based on our observations regarding the range of the damping constants of low-frequency modes.

This technique is implemented on the simulated signal. The DFT of the artificial closure sound is obtained (dashed line in Fig. 4), components of the complex DFT above 140 Hz are zeroed, and an inverse DFT is obtained. When the Prony method is applied to this signal, an SER of 40 dB is obtained. A signal is then reconstructed using the estimated modes with center frequencies below 90 Hz and this signal is subtracted from the original artificial signal. The DFT of this signal is given in Fig. 4 (solid line). We refer to this new artificial signal as the modal high-pass filtered signal. In Fig. 5, this filtration technique is shown in a block diagram. When the Prony method is applied to the modal high-pass filtered signal, the frequencies and energies of the modes above 90 Hz are found with an accuracy of $< 2\%$ for frequencies and $< 16\%$ for energies (Table IV). An SER of 14 dB is obtained in this case.

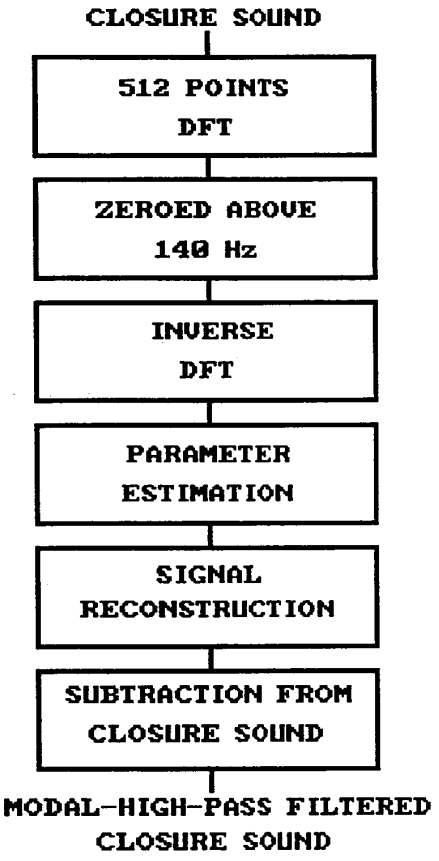

Fig. 5. Block diagram of modal high-pass filtering.

The error levels obtained in this highly idealized simulation are difficult to attain in the study of actual signals. First of all, such a high SER_K (40 dB) is not always possible in the estimation of low-frequency components. Furthermore, model order determination is still prone to errors, hence additional variation in parameter estimates is expected. When the noise level is increased so that the SNR is decreased to 21 dB from 22.5 dB, it is observed that the three high-frequency modes can still be estimated with errors less than 4.2% in frequency and 26% in energy, while a reliable order determination can still be done at 12.4 dB SER_K. If the SNR is further decreased to 20 dB, the maximum error in frequency and energy becomes 5.2% and 28%, respectively, but choosing the correct order according to the above procedure is not possible. Obviously, these figures are dependent on the number of modes included, on the relative energy of each mode, and on the noise level. For comparison purposes, 5% estimation error for frequencies and 25% error for energies are taken as the limitations of the whole identification procedure.

The modal high-pass filtering technique can be summarized as follows:

1) The DFT of the heart sound is calculated.
2) The DFT is zeroed above 140 Hz.
3) The inverse DFT is applied.
4) The Prony method is used to estimate the parameters of this low-pass filtered signal.

TABLE IV
ESTIMATED PARAMETERS OF THE MODAL HIGH-PASS FILTERED ARTIFICIAL CLOSURE SOUND. ONLY THE PARAMETERS OF THE MODES WHICH HAVE MORE THAN 1% NORMALIZED ENERGIES ARE GIVEN

fre	damp	ampl	phase	energy
100.2	80.2	605.9	4.271	1.000
169.8	115.8	458.4	0.068	0.443
288.3	241.9	120.3	1.218	0.013

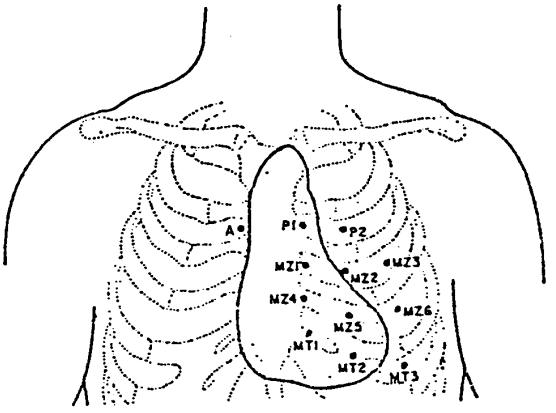

Fig. 6. Twelve recording sites on the surface of the chest.

5) A signal is reconstructed using the parameters of modes with less than 90 Hz center frequency.
6) This constructed signal is subtracted from the original signal to obtain the modal high-pass filtered signal.

III. RESULTS

A. Data

Recordings are examined from 10 patients who have a St. Jude-type bileaflet mechanical heart valve prosthesis in aortic position. Ages of the patients are between 18 and 40. Patients 3 and 9 are female and the others are male. Diameters of the prostheses are 21–27 mm. Recordings are made two or six months following the implantation of the prosthesis.

B. Site-to-Site Variation of the Second Heart Sounds

To observe the site-to-site parameter variation of the second heart sounds, 12 recording sites are selected on the surface of the chest. These recording sites are illustrated in Fig. 6. The anatomical definitions of these points are as follows:

A: Intersection point of second intercostal space with right sternal border.

P1: Intersection point of second intercostal space with left sternal border.

P2: In the second intercostal space, mid point between P1 and intersection point of second intercostal space with left medio-clavicular line.

MZ1: Intersection point of third intercostal space with left sternal border.

MZ2: In the third intercostal space, mid point between MZ1 and MZ3.

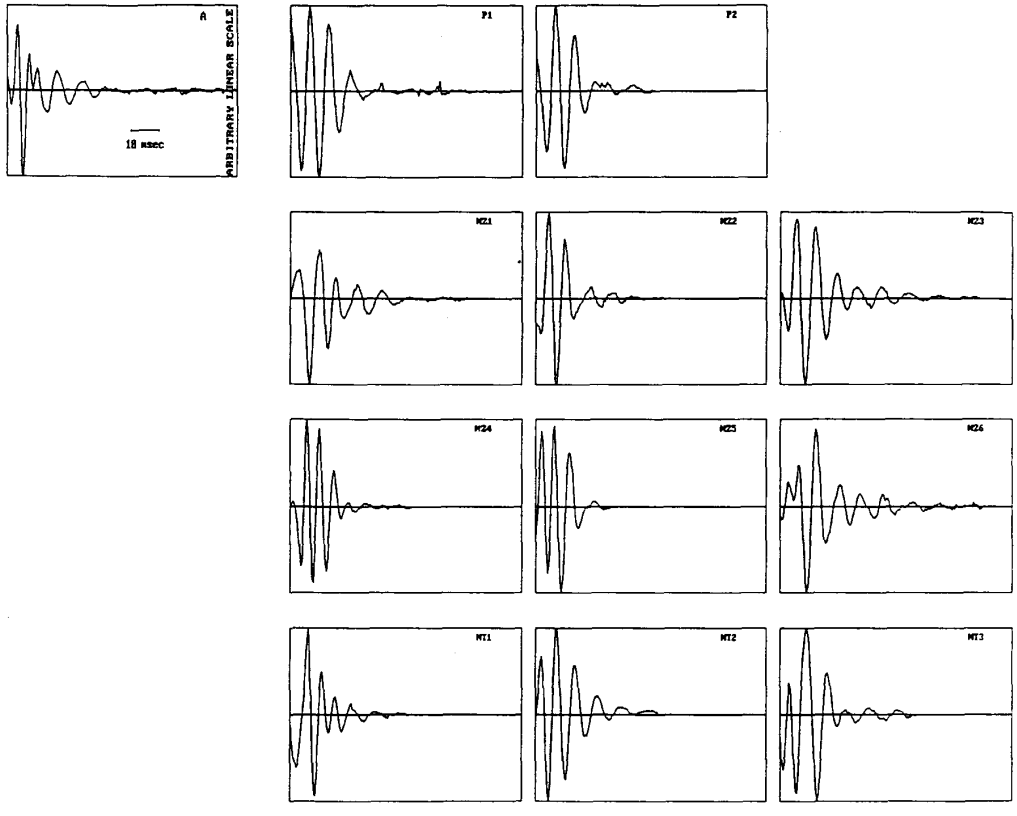

Fig. 7. Averaged closure sounds recorded at 12 different sites.

MZ3: Intersection point of the third intercostal space with the left medio-clavicular line.

MZ4: Intersection point of fourth intercostal space with left sternal border.

MZ5: In the fourth intercostal space, mid point between MZ4 and MZ6.

MZ6: Intersection point of the fourth intercostal space with the left medio-clavicular line.

MT1: Intersection point of fifth intercostal space with left sternal border.

MT2: In the fifth intercostal space, mid point between MT1 and MT3.

MT3: Intersection point of the fifth intercostal space with the left medio-clavicular line.

A, P1, MZ1, and MT3 are the classical auscultation sites which are called aortic, pulmonary, mesocardiac, and mitral auscultation sites, respectively.

In Fig. 7, second heart sounds recorded at 12 different sites for the third patient are given. These signals are high-pass filtered signals using the modal filtration technique described in Section II-B2). It can be seen that the temporal variation of these signals is different from site-to-site.

These sounds are then analyzed as explained above. For each recording site, model parameters are estimated. For 10 patients, parameters of modes with significant energies (more than 10% normalized energy) are given in Table V. It is possible to classify the modes, with respect to the frequencies, into different groups. For this purpose, the Average Linkage Method is used [18]. This method uses the Euclidean distance between data (or data groups). In each step, the distances of all possible pairs of data (or data groups) are calculated. The pair of data (or data groups) with the smallest distance constitutes a new group and the number of groups is decreased by one. The algorithm stops when the number of groups is decreased to the number initially given. Using this method in each patient, 4–5 groups are identified with different means. Then, means and coefficient of variations (ratio of the standard deviation to the group mean) of each group for all patients are computed (Table VI). In this table, the coefficient of variations do not exceed 5% in any of the mode groups.

It can be observed in Table V that in each patient energies of modes change from site-to-site. In order to compare energies of modes between different sites, for each patient the ratios $E_2/E_1, E_3/E_1$, and E_4/E_1 are calculated for each recording site. It can be seen from Table V that, for several recording sites, Mode 1 (modes with the frequency of about 110 Hz) does not exist. So, energy of this mode can be accepted as zero. However, for computation of the above-given energy ratios, assigning zero to E_1 yields infinity and makes statistical comparison impossible. For this reason, it is necessary to assign a value to the denominators of the energy ratios which are zero, so that statistical comparison is possible. For this

TABLE V
(a) ESTIMATED PARAMETERS OF PATIENT 1. (b) ESTIMATED PARAMETERS OF PATIENT 2

A

fre	damp	phase	energy
104.8	55.1	0.779	0.229
150.8	111.2	-0.836	1.000
226.1	226.1	2.592	0.617

P1

fre	damp	phase	energy
107.3	46.5	1.460	1.000
140.3	116.0	-0.790	0.399

P2

fre	damp	phase	energy
107.6	72.8	2.719	1.000
138.1	124.5	-0.500	0.433

MZ1

fre	damp	phase	energy
107.1	39.3	-0.745	1.000
144.7	79.2	2.406	0.422

MZ2

fre	damp	phase	energy
138.5	127.8	0.776	1.000

MZ3

fre	damp	phase	energy
109.0	121.4	1.180	0.664
131.6	106.1	4.371	1.000

MZ4

fre	damp	phase	energy
103.6	52.0	3.108	0.339
144.9	72.4	4.584	1.000
189.9	101.5	0.822	0.781

MZ5

fre	damp	phase	energy
133.7	134.3	0.124	0.655
183.2	235.3	3.638	1.000

MZ6

fre	damp	phase	energy
108.4	140.8	0.087	0.167
141.2	117.6	2.821	1.000
169.2	72.4	-0.168	0.126

MT1

fre	damp	phase	energy
109.4	107.5	2.570	1.000
135.6	128.1	2.835	0.892

MT2

fre	damp	phase	energy
97.5	82.8	-0.523	1.000

MT3

INVALID

(a)

A

INVALID

P1

fre	damp	phase	energy
108.1	41.3	0.893	1.000
135.1	60.4	1.604	0.810
177.7	126.6	3.914	0.716

P2

fre	damp	phase	energy
104.5	99.8	3.622	1.000
175.1	98.8	-0.184	0.532

MZ1

INVALID

MZ2

fre	damp	phase	energy
165.9	144.4	4.447	1.000

MZ3

fre	damp	phase	energy
106.0	121.4	2.016	0.563
163.6	106.0	-1.121	1.000

MZ4

fre	damp	phase	energy
123.3	87.3	0.544	1.000
161.4	143.4	2.488	0.650

MZ5

fre	damp	phase	energy
105.7	75.3	0.435	1.000
175.6	106.2	1.421	0.826
211.1	168.8	3.399	0.292

MZ6

fre	damp	phase	energy
162.9	94.8	1.647	1.000
195.0	192.8	-1.562	0.300

MT1

INVALID

MT2

fre	damp	phase	energy
104.5	49.9	1.217	1.000
144.3	29.5	0.664	0.296

MT3

fre	damp	phase	energy
125.3	112.8	1.175	1.000
179.0	108.8	3.339	0.429
250.0	142.9	4.457	0.255

(b)

TABLE V (*Cont.*)
(c) ESTIMATED PARAMETERS OF PATIENT 3. (d) ESTIMATED PARAMETERS OF PATIENT 4

A				P1				P2			
fre	damp	phase	energy	fre	damp	phase	energy	fre	damp	phase	energy
121.7	78.8	4.642	0.538	141.7	137.9	0.648	1.000	140.6	162.3	0.687	1.000
228.3	253.0	3.673	1.000	181.5	172.1	3.783	0.378	177.2	177.5	3.795	0.423
301.4	216.5	4.265	0.440								

MZ1				MZ2				MZ3			
fre	damp	phase	energy	fre	damp	phase	energy	fre	damp	phase	energy
134.8	99.6	-1.177	0.260	126.5	144.4	3.944	0.474	133.7	95.9	2.478	1.000
175.7	242.3	1.490	1.000	177.1	189.6	1.327	1.000	178.0	227.7	0.576	0.576
229.9	183.6	3.097	0.199	222.5	189.7	-1.537	0.278				

MZ4				MZ5				MZ6			
fre	damp	phase	energy	fre	damp	phase	energy	fre	damp	phase	energy
182.9	148.2	1.356	0.337	168.4	249.3	-0.128	1.000	129.4	85.1	2.445	0.809
229.6	221.6	3.905	1.000	213.9	290.1	2.707	0.871	171.1	306.6	-0.633	1.000
								211.3	178.2	2.558	0.531

MT1				MT2				MT3			
fre	damp	phase	energy	fre	damp	phase	energy	fre	damp	phase	energy
126.7	117.4	0.546	0.320	128.1	75.2	1.138	0.308	139.3	101.0	3.427	1.000
186.0	128.0	4.019	0.865	168.9	186.2	4.310	1.000	172.1	123.1	0.267	0.318
234.2	147.4	-0.083	1.000								

(c)

A				P1				P2			
fre	damp	phase	energy					fre	damp	phase	energy
110.6	102.0	-0.427	0.626	INVALID				107.1	64.6	4.380	1.000
170.9	145.6	1.483	1.000					141.1	64.9	4.341	0.153

MZ1				MZ2				MZ3			
fre	damp	phase	energy	fre	damp	phase	energy	fre	damp	phase	energy
119.2	106.2	1.146	0.169	144.1	140.9	1.722	0.174	145.3	83.8	4.316	0.501
185.2	173.7	4.410	1.000	207.3	132.8	3.866	1.000	180.5	137.5	0.967	1.000
232.0	250.5	0.193	0.457	251.7	230.0	-1.098	0.809				

MZ4				MZ5				MZ6			
fre	damp	phase	energy	fre	damp	phase	energy	fre	damp	phase	energy
111.6	165.3	3.521	1.000	107.3	85.7	2.843	1.000	131.0	130.7	3.603	1.000
219.1	115.1	3.298	0.122	150.7	142.7	-0.818	0.124				
				249.3	235.2	-1.397	0.114				

MT1				MT2				MT3			
fre	damp	phase	energy	fre	damp	phase	energy	fre	damp	phase	energy
109.8	70.8	3.593	0.230	117.7	126.5	1.714	1.000	105.2	157.0	2.637	1.000
155.6	96.3	-0.993	1.000	206.9	175.6	4.415	0.536	225.0	223.3	4.526	0.484
225.4	171.2	-0.542	0.926								

(d)

TABLE V (*Cont.*)
(e) ESTIMATED PARAMETERS OF PATIENT 5. (f) ESTIMATED PARAMETERS OF PATIENT 6

A

fre	damp	phase	energy
99.3	68.6	-0.103	1.000
161.0	77.6	0.761	0.740
197.0	130.6	3.338	0.269

P1

fre	damp	phase	energy
104.1	93.0	4.299	0.478
168.9	138.6	1.498	1.000

P2

fre	damp	phase	energy
178.5	167.2	2.400	1.000

MZ1

fre	damp	phase	energy
112.6	143.1	1.718	0.269
162.8	240.2	4.091	1.000
278.1	295.5	2.616	0.235

MZ2

fre	damp	phase	energy
205.7	199.7	2.155	1.000

MZ3

fre	damp	phase	energy
112.3	159.5	4.307	1.000
160.4	116.9	0.250	0.388

MZ4

fre	damp	phase	energy
112.1	95.6	1.188	0.973
160.6	220.2	0.260	1.000

MZ5

fre	damp	phase	energy
110.6	83.3	1.033	1.000

MZ6

fre	damp	phase	energy
111.6	103.7	-0.608	0.360
135.1	83.6	2.688	1.000
197.1	156.2	-1.515	0.196

MT1

fre	damp	phase	energy
159.0	85.9	3.485	1.000
206.0	174.5	0.655	0.639

MT2

fre	damp	phase	energy
109.2	154.6	-0.605	1.000
166.3	139.7	3.236	0.326

MT3

fre	damp	phase	energy
104.7	73.0	-0.286	0.476
130.1	55.0	2.838	1.000
202.7	127.2	1.230	0.531
255.4	249.6	4 457	0.552

(e)

A

fre	damp	phase	energy
130.1	131.0	0.275	1.000
183.6	100.6	4.688	0.313

P1

fre	damp	phase	energy
92.7	92.2	0.958	0.176
142.0	179.6	-1.245	1.000

P2

fre	damp	phase	energy
96.9	36.0	4.663	0.111
142.8	122.1	-0.255	1.000
194.3	168.7	2.736	0.671

MZ1

fre	damp	phase	energy
142.5	170.3	4.429	1.000
201.6	154.5	1.526	0.581

MZ2

INVALID

MZ3

fre	damp	phase	energy
99.0	136.2	3.314	1.000
138.4	119.6	0.983	0.573

MZ4

fre	damp	phase	energy
102.9	62.0	0.137	0.119
145.3	217.0	4.312	1.000
196.4	164.6	1.365	0.717

MZ5

fre	damp	phase	energy
106.0	130.0	4.207	1.000
138.8	102.9	0.597	0.174

MZ6

fre	damp	phase	energy
97.7	139.2	2.344	1.000
132.5	159.3	-0.248	0.740

MT1

fre	damp	phase	energy
132.9	192.0	-0.706	1.000
205.8	158.3	4.450	0.674

MT2

fre	damp	phase	energy
100.3	166.3	2.625	1.000
202.5	121.5	0.435	0.288

MT3

fre	damp	phase	energy
135.7	191.7	1.077	1.000
203.4	164.0	3.921	0.745

(f)

TABLE V (*Cont.*)
(g) ESTIMATED PARAMETERS OF PATIENT 7. (h) ESTIMATED PARAMETERS OF PATIENT 8

A				P1				P2			
fre	damp	phase	energy	fre	damp	phase	energy	fre	damp	phase	energy
98.1	140.6	1.887	1.000	150.7	210.5	0.285	1.000	154.2	152.3	1.549	0.416
153.7	206.0	-1.460	0.335					242.2	288.4	2.447	1.000

MZ1				MZ2				MZ3			
fre	damp	phase	energy	fre	damp	phase	energy	fre	damp	phase	energy
90.0	211.9	0.319	1.000	138.0	151.2	4.455	1.000	192.1	129.6	1.287	1.000
145.9	176.7	2.355	0.775	210.4	244.9	-0.416	0.983				

MZ4				MZ5				MZ6			
fre	damp	phase	energy	fre	damp	phase	energy	fre	damp	phase	energy
138.4	178.6	0.857	0.596	137.3	207.5	-0.507	1.000	157.0	112.7	1.481	1.006
191.4	211.7	3.018	1.000	179.0	176.5	3.066	0.720	194.6	117.9	4.303	0.219
246.7	256.0	-1.563	0.167								

MT1				MT2				MT3			
fre	damp	phase	energy	fre	damp	phase	energy	fre	damp	phase	energy
90.6	107.4	0.936	0.804	143.6	156.8	2.917	1.000	146.8	119.2	1.675	1.000
148.6	269.3	3.241	1.000	183.8	93.4	0.051	0.760	173.8	97.4	-0.345	0.755
183.0	83.7	0.637	0.231								
231.9	198.0	-0.385	0.205								

(g)

A				P1				P2			
fre	damp	phase	energy	fre	damp	phase	energy	fre	damp	phase	energy
99.8	78.6	3.897	1.000	104.5	55.5	3.014	0.647	133.0	42.6	4.426	0.210
213.5	100.2	2.646	0.479	134.9	57.7	3.793	0.169	187.9	107.4	-0.956	1.000
				205.7	112.2	3.762	1.000				

MZ1				MZ2				MZ3			
fre	damp	phase	energy	fre	damp	phase	energy	fre	damp	phase	energy
143.4	172.2	-0.593	0.490	107.1	94.0	1.902	0.742	105.6	79.0	-0.763	0.805
192.1	262.7	2.338	1.000	144.2	89.8	1.225	1.000	174.5	97.1	2.068	1.000
				181.0	96.5	2.889	0.615	224.9	83.7	4.007	0.283

MZ4				MZ5				MZ6			
fre	damp	phase	energy	fre	damp	phase	energy	fre	damp	phase	energy
108.8	86.8	1.824	1.000	142.1	101.6	0.806	1.000	110.8	76.7	3.903	1.000
132.1	84.8	-0.287	0.507	184.9	93.0	3.699	0.239	149.8	120.8	0.446	0.384

MT1				MT2				MT3			
fre	damp	phase	energy	fre	damp	phase	energy	fre	damp	phase	energy
101.3	49.5	0.706	1.000	110.1	183.4	3.728	0.758	104.5	120.3	4.616	0.745
132.1	39.5	3.060	0.178	140.4	110.8	0.548	1.000	143.7	170.0	0.942	1.000
198.4	47.0	-0.793	0.137								

(h)

TABLE V (*Cont.*)
(i) ESTIMATED PARAMETERS OF PATIENT 9. (j) ESTIMATED PARAMETERS OF PATIENT 10

A				P1				P2			
fre	damp	phase	energy	fre	damp	phase	energy	fre	damp	phase	energy
110.8	170.1	1.234	0.545	190.1	182.7	-0.106	1.000	108.1	81.0	4.153	0.723
166.9	194.3	1.298	1.000	231.9	236.7	2.955	0.715	181.6	127.8	4.662	1.000

MZ1				MZ2				MZ3			
fre	damp	phase	energy	fre	damp	phase	energy	fre	damp	phase	energy
111.1	163.0	4.158	0.405	107.6	136.3	3.093	1.000	115.9	87.6	3.063	1.000
179.9	142.1	-0.479	1.000	176.3	172.7	4.263	0.219	168.2	103.6	3.921	0.923
								217.9	205.3	0.353	0.931

MZ4				MZ5				MZ6			
fre	damp	phase	energy	fre	damp	phase	energy	fre	damp	phase	energy
114.4	186.5	2.093	0.904	102.1	58.2	2.150	0.423	184.4	172.1	2.697	1.000
171.8	179.1	4.549	1.000	221.1	181.6	2.083	1.000	238.9	170.4	0.150	0.311
252.3	279.3	0.164	0.258								

MT1				MT2				MT3			
fre	damp	phase	energy	fre	damp	phase	energy	fre	damp	phase	energy
108.5	149.9	3.620	1.000	101.7	80.3	-0.199	1.000	110.9	102.9	-0.327	1.000
181.8	238.3	-0.430	0.429	139.3	159.3	0.723	0.275	170.5	199.5	2.234	0.558
				186.8	178.9	2.882	0.626				

(i)

A				P1				P2			
fre	damp	phase	energy	fre	damp	phase	energy	fre	damp	phase	energy
92.3	84.0	3.346	1.000	144.1	94.4	-0.692	1.000	141.7	109.9	1.108	1.000

MZ1				MZ2				MZ3			
				fre	damp	phase	energy	fre	damp	phase	energy
INVALID				94.0	72.2	2.467	0.386	138.0	87.8	-0.602	0.301
				134.0	115.5	-0.258	1.000	170.5	177.6	3.499	1.000
				176.0	192.3	3.021	0.819				

MZ4				MZ5				MZ6			
fre	damp	phase	energy	fre	damp	phase	energy	fre	damp	phase	energy
140.5	132.2	3.234	1.000	132.3	190.1	-1.330	1.000	141.2	176.7	-0.487	1.000

MT1				MT2				MT3			
fre	damp	phase	energy	fre	damp	phase	energy	fre	damp	phase	energy
184.2	159.7	-0.784	1.000	96.7	167.2	1.080	0.402	100.2	55.0	0.271	0.166
223.9	238.0	2.833	0.606	182.4	172.0	3.532	1.000	180.7	191.6	3.811	1.000
								215.0	218.0	3.765	0.569

(j)

TABLE VI
MEANS (HZ) AND COEFFICIENT OF VARIATIONS (IN PARENTHESES, %) OF MODAL FREQUENCIES FOR THE PATIENTS. THE GROUPS FOR WHICH COEFFICIENT OF VARIATIONS ARE NOT GIVEN CONSIST OF ONLY ONE ELEMENT

	MODE1	MODE2	MODE3	MODE4	MODE5
PAT1	106(3)	140(4)	188(2)	226	
PAT2	106(3)	132(5)	170(4)	203(4)	250
PAT3	132(5)	177(3)	224(4)	301	
PAT4	111(4)	145(5)	179(4)	207(0)	233(5)
PAT5	109(4)	133(3)	165(4)	202(2)	267(5)
PAT6	99(4)	139(3)	198(4)		
PAT7	94(4)	147(5)	185(4)	210	240(3)
PAT8	106(3)	140(4)	184(3)	211(5)	
PAT9	109(4)	139	178(4)	220(1)	240(4)
PAT10	103(3)	137(3)	178(3)	219(2)	

purpose, a value of 20 is assigned to the above-mentioned energy ratios. It should be emphasized that statistical analyses results do not change when this value is chosen between 10–100.

In Table VII, means and standard deviations of energy ratios are given for 12 different recording sites. It can be observed from this table that means of energy ratios vary from site-to-site. To observe if the variation of energy ratios on the surface of the chest is statistically significant, we first used the one-way analysis of variance test. As a result of this test, no significant difference is observed (Table VIII). The analysis of variance test gives information about the variation of overall data and a significant difference between several pairs of groups may be suppressed. According to the resonant structure hypothesis, energies of modes will vary depending on the distance of recording sites to the related anatomical structures. However, it does not imply that energy ratios will be different in each recording site. In fact, according to this hypothesis, energy ratios may be the same at adjacent recording sites which are close to the same part of the heart. As a result of the analysis of variance test, similarity of energy ratios at adjacent recording sites may suppress the significant difference between several recording sites. Therefore, energy ratios are also analyzed by using a t-test to observe if there are significantly different pairs of recording sites. The significance level for t-tests is chosen as $p < 0.01$. As a result, E_2/E_1 and E_4/E_1 are found to be significantly higher at MZ2 with respect to MT2 ($p < 0.01$). When the significance level for the t-test is accepted as $p < 0.05$, additional significantly different pairs of recording sites are observed. In Table IX, these recording sites are given. It can be observed from this table that the energy ratios E_2/E_1 and E_4/E_1 are found to be significantly higher for MZ2 with respect to several other recording sites.

TABLE VII
MEAN AND STANDARD DEVIATION OF ENERGY RATIOS OBTAINED FOR DIFFERENT RECORDING SITES

	E_2/E_1	E_3/E_1	E_4/E_1
A	2.9(6.5)	3.2(7.0)	2.9(6.5)
P1	4.8(4.5)	3.3(4.6)	2.7(7.0)
P2	6.3(5.1)	3.6(4.9)	1.2(2.9)
MZ1	5.9(5.1)	3.1(4.1)	6.7(9.9)
MZ2	7.7(3.9)	4.6(4.9)	11.4(9.9)
MZ3	4.0(4.9)	4.5(4.8)	0.2(0.3)
MZ4	6.2(4.8)	4.2(4.9)	4.6(8.3)
MZ5	3.4(4.9)	4.6(5.1)	5.8(9.7)
MZ6	5.6(4.8)	4.4(5.2)	3.5(7.4)
MT1	5.2(5.3)	3.5(5.0)	8.0(9.9)
MT2	2.5(4.3)	2.4(4.1)	0.1(0.2)
MT3	5.2(5.1)	4.6(4.9)	2.9(7.0)

TABLE VIII
p VALUES AS A RESULT OF THE ONE-WAY ANALYSIS OF VARIANCE TEST FOR THE ENERGY RATIOS

E_2/E_1	E_3/E_1	E_4/E_1
0.29	0.47	0.19

TABLE IX
IN EACH PAIR, ENERGY RATIO OF THE FIRST RECORDING SITE IS FOUND TO BE SIGNIFICANTLY HIGHER WITH RESPECT TO THE SECOND RECORDING SITE ($p < 0.05$). THE PAIRS WHICH ARE SIGNIFICANTLY DIFFERENT FOR $p < 0.01$ ARE MARKED BY (*)

E_2/E_1	E_3/E_1	E_4/E_1
MZ2-A	———	MZ2-A
MZ2-MZ3		MZ2-P1
MZ2-MZ5		MZ2-P2
MZ2-MT2*		MZ2-MZ3
		MZ2-MZ6
		MZ2-MT2*
		MZ2-MT3
		MT1-MZ3
		MT1-MT2
		MZ1-MT2

IV. CONCLUSION

Heart sound signal as recorded on the surface of the chest is related to its generation mechanism in a very complex manner. The work presented in this paper describes a methodology for identifying a model which emerges from the hypothesis that a closure sound of a mechanical prosthesis is the output a linear system of acoustic resonating structures excited by a short pulse generated during rapid deceleration of valve occluder [12]. This acoustic system, made up of the heart, its partitions, and major vessels, is a highly complex system containing many coupled elements. The task of identification is further complicated by noise and measurement problems. These problems have been addressed in this paper on a quantitative basis, both by simulation and by analysis of real signals. It is demonstrated that the number of modes necessary

to model the system varies with noise, even after the Akaike Criterion is met; the identification of mode parameters is highly dependent on noise level; and for correct estimation of parameters of modes of interest, it is necessary to employ a sophisticated technique to reduce the effect of the low-frequency–high-energy modes.

It is observed that the coefficient of variation of modal frequencies in any of the patients does not exceed 5% over the surface of the chest when the methodology presented in this paper, i.e., signal averaging, modal high-pass filtering and the given order selection method, is employed. This variation is within the accuracy limits of the method. Therefore, the hypothesis of resonant acoustic structures is strongly supported by this result. Furthermore, in line with the implications of the same hypothesis, it is found that relative energies of resonance modes vary across the chest surface. Although a consistent pattern of variation is not found, statistical analyses have shown that two sites are significantly different with respect to their energy ratios E_2/E_1 and E_4/E_1 ($p < 0.01$, $N = 10$).

Application of the proposed method to different patient populations and correlation of mode parameters to the position and physical dimensions of the internal structures can be helpful in associating a particular mode to a particular structural element. For example, patients with left ventricular dilatation or other cases where the volumes of different partitions in the heart or vessels are known to be altered should have shifted mode frequencies compared to normals. The study of such patients will help establish the relation between modal parameters and the structures.

ACKNOWLEDGMENT

The authors wish to thank Prof. S. Yücemen for valuable advice during the statistical analysis of data.

REFERENCES

[1] J. C. Hylen, F. E. Kloster, R. H. Herr, A. Starr, and H. E. Griswold, "Sound spectrographic diagnosis of aortic ball variance," *Circ.*, vol. 39, pp. 849–858, June 1969.

[2] R. F. Gordon, M. Najimi, B. Kingsley, B. L. Segal, and J. W. Linhart, "Spectroanalytic evaluation of aortic prosthetic valves," *Chest*, vol. 66, pp. 44–49, July 1974.

[3] Y. Kagawa, S. Nitta, M. Tanaka, and T. Horiouchi, "Real-time sound spectroanalysis for diagnosis of malfunctioning prosthetic valves," *J. Thorac. Cardiovasc. Surg.*, vol. 79, pp. 671–679, 1980.

[4] P. D. Stein, H. N. Sabbah, J. B. Lakier, and D. J. Magilligan, "Frequency of the first heart sound in the assessment of the stiffening of mitral bioprosthetic valves," *Circ.*, vol. 63, pp. 200–203, Jan. 1981.

[5] P. D. Stein, H. N. Sabbah, J. B. Lakier, and S. R. Kemp, "Frequency spectra of the first heart sound and of the aortic component of the second heart sound in patients with degenerated porcine bioprosthetic valves," *Amer. J. Cardiol.*, vol. 53, pp. 557–561, Feb. 1984.

[6] L. G. Durand, M. B. Blanchard, G. Cloutier, H. N. Sabbah, and P. D. Stein, "Comparison of pattern recognition methods for computer-assisted classification of spectra of heart sounds in patients with a porcine bioprosthetic valve implanted in the mitral position," *IEEE Trans. Biomed. Eng.*, vol. BME-37, pp. 1121–1129, Dec. 1987.

[7] R. J. Adolph, J. F. Stephens, and K. Tanaka, "The clinical value of frequency analysis of the first heart sound in myocardial infarction," *Circ.*, vol. 41, pp. 1003–1014, June 1970.

[8] W. B. Clarke, S. M. Austin, P. M. Shah, and P. M. Griffen, "Spectral energy of the first heart sound in acute myocardial ischemia," *Circ.*, vol. 57, pp. 593–598, Mar. 1978.

[9] J. Semmlow, W. Welkowitz, J. Kostis, and J. W. Mackenzie, "Coronary artery disease—Correlates between diastolic auditory characteristic and coronary artery stenoses," *IEEE Trans. Biomed. Eng.*, vol. BME-30, pp. 136–139, Feb. 1983.

[10] P. J. Arnott, G. W. Pfeiffer, and M. E. Tavel, "Spectral analysis of heart sounds: Relationships between some physical characteristics and frequency spectra of first and second heart sounds in normals and hypertensives," *J. Biomed. Eng.*, vol. 6, pp. 121–128, Apr. 1984.

[11] M. Akay, J. L. Semmlow, W. Welkowitz, M. D. Bauer, and J. B. Kostis, "Detection of coronary occlusions using autoregressive modeling of diastolic heart sounds," *IEEE Trans. Biomed. Eng.*, vol. 37, pp. 366–373, Apr. 1990.

[12] H. Köymen, B. K. Altay, and Y. Z. İder, "A study of prosthetic heart valve sounds," *IEEE Trans. Biomed. Eng.*, vol. BME-34, pp. 853–863, Nov. 1987.

[13] D. L. Sikarskie, P. D. Stein, and M. Vable, "A mathematical model for aortic valve vibration," *J. Biomechan.*, vol. 17, pp. 831–837, 1984.

[14] F. Meno, P. S. Reddy, and L. Bernardi, "Heart sound propagation in the human thorax," *Clin. Phys. Physiol. Meas.*, vol. 6, pp. 123–129, 1985.

[15] S. M. Kay and L. Marple, "Spectrum analysis—A modern perspective," *Proc. IEEE*, vol. 69, pp. 1380–1419, Nov. 1981.

[16] H. Akaike, "A new look at the statistical model identification," *IEEE Trans. Automat. Contr.*, vol. AC-19, pp. 716–723, Dec. 1974.

[17] M. E. Tavel, *Clinical Phonocardiography and External Pulse Recording*. Chicago: Year Book Med. Publ., 1985, p. 15.

[18] R. A. Johnson and D. W. Wichern, *Applied Multivariate Statistical Analysis*. Englewood Cliffs, NJ: Prentice-Hall, 1982, p. 552.

Ahmet Baykal was born in K. Maras, Turkey on September 27, 1961. He received the M.D. degree from Aegean University in 1984 and the Ph.D. degree in biomedical engineering from Middle East Technical University in 1992. He did postdoctoral studies at the Biomedical Engineering Department of The Johns Hopkins University between 1993 and 1994.

His main research areas are biomedical signal processing, modeling and analysis of phonocardiogram, and electrophysiology of ventricular fibrillation and cardio-pulmonary resuscitation.

Y. Ziya İder was born in Erzincan, Turkey, on October 9, 1951. He received the B.Sc. degree in electrical engineering from Middle East Technical University in 1973, the M.Sc. degree in biomedical engineering from the University of Southern California in 1976, and the Ph.D. degree in biomedical engineering from Northwestern University in 1979.

In 1979, he joined the Department of Electrical and Electronics Engineering of Middle East Technical University, where he is currently employed as a Professor. His main research areas are acquisition and processing of bioelectric and other physiological signals, electrical impedance tomography, and magnetic resonance imaging.

Hayrettin Köymen (S'74–M'87–SM'91) was born in Ankara, Turkey, on June 7, 1952. He received B.Sc. and M.Sc. degrees from Middle East Technical University, Ankara, Turkey, in 1973 and 1976, respectively, and the Ph.D. degree from the University of Birmingham, England, in 1979, all in electrical engineering.

In 1979, he became a faculty member of the Middle East Technical University. Until 1982, his work involved underwater acoustics and oceanographic instrumentation. Since 1982, his work has involved physiological signal acquisition and processing, medical ultrasonics, and ultrasonic nondestructive evaluation. In 1990, he joined the faculty of Bilkent University, Ankara, where he is now a Professor in the Department of Electrical and Electronics Engineering. His current research interests are personal computer-based biomedical signal acquisition and processing, medical imaging, finite amplitude effects in medical ultrasonics, and acoustic microscopy using leaky waves in layered media.